EVIDENCE OF SEASONALLY DEPENDENT STRATOSPHERE-TROPOSPHERE EXCHANGE AND PURGING OF LOWER STRATOSPHERIC AEROSOL FROM A MULTI-YEAR LIDAR DATASET

Robert T. Menzies

David M. Tratt

Jet Propulsion Laboratory

California Institute of Technology

Pasadena, CA 91109

U.S.A.

Tel: 1-818-354-3787

March, 1994

EVIDENCE OF SEASONALLY DEPENDENT STRATOSPHERE-TROPOSPHERE EXCHANGE AND PURGING OF LOWER STRATOSPHERIC AEROSOL FROM A MULTI-YEAR LIDAR DATASET

R.T. Menzies and D.M. Tratt

Abstract

Troposphericand lower stratospheric aerosol backscatter dataobtainedfrom a calibrated backscatter lidar at Pasadena, California (34° N latitude) over the 1984-1993 period clearly indicate tightly coupled aerosol optical properties in the upper troposphere and lower stratosphere in the winter and early spring, due to the active mid-latitude stratospheric-tropospheric (ST) exchange processes occurring atthistime ofyear. Lidar data indicate that during pre-Pinatubo background conditions, the subsequent purging of the aerosol in the upper troposphere caused a significant reduction in the aerosol content throughout the 8-18 km altitude region in the early spring period. The post-Pinatubo evidence of intense exchange in the winter and early spring is a significant increase in the upper tropospheric aerosol content, such that the backscatter levels reach values nearly equivalent to the enhanced backscatter levels existing in the lower stratosphere. The calculated stratospheric mass extrusion rate is consistent with a 45-day lifetime of lower stratospheric aerosol during this part of the year, which implies that mid-latitude ST exchange is a significant sink for stratospheric aerosol.

1. Introduction

The study of seasonal and multi-year behavior of aerosol distributions as a function of altitude in the troposphere and lower stratosphere can be used in assessments of stratosphere-troposphere (ST) exchange and the efficacy of certain sources and sinks for the aerosol particles. We report here a study based largely on measurements of vertical profiles of aerosol backscatter over a period between 1985 and 1993, a period which includes very clean, background conditions in the lower stratosphere as well as the extreme volcanic conditions produced by the Mount Pinatubo eruption in mid-1991.

The mixing of stratospheric aerosols into the troposphere through ST exchange processes occurring at extratropical latitudes can significantly affect the residence times and altitude distributions of the aerosols. Particularly in extreme volcanic conditions (such as the present time) the aerosols themselves have potential climate impacts, due to the direct radiative forcing of the stratospheric aerosols [Lacis, et al., 1992] as well as the aerosol impact on cirrus formation and the consequent alteration of cirrus radiative properties [Sassen, 1992; Jensen and Toon, 1992]. In non-volcanic or background conditions, the aerosols remain useful as tracers of mass exchange.

Mass exchange processes were discussed in the 1960's, using radioactive debris to trace air masses of stratospheric origin [Staley, 1962; Danielsen, 1968], and aircraft instrumented with sensors of ozone and meteorological variables were used on several occasions in the succeeding decades to study in ever greater detail the tropopause fold mechanism for the downward transport of stratospheric air masses and the exchange of constituents between the stratosphere and troposphere at extratropical latitudes [Danielsen and Mohnen, 1977; Shapiro, 1980; Danielsen et al., 1987; Browell et al., 1987; Russell et al., 1991]. Radioactive debris collected at surface stations over a wide range of latitudes in the northern hemisphere indicated a seasonal variability, with a spring maximum and autumn minimum [Staley, 1962], This was linked to large-scale cyclogenesis in the winter and early spring, and the development of upper-level baroclinic waves in the tropospheric jet stream, with deep convection also maximized in the troposphere in the early spring. The aforementioned aircraft experiments all occurred during the spring months over the western or Midwestern U. S., taking advantage of the tendency for large-scale cyclonic flow of the jet stream over this area during these months and the corresponding high probability of major tropopause fold events.

Early attempts to assess the ST mass exchange budget on a global scale utilized the surface radioactive debris data along with the occasional aircraft case studies and extrapolations based on estimates of global cyclonic activity and general characteristics of the large-scale circulation. Reiter [1975] reported a budget estimate of the various mechanisms which are chiefly responsible for the annual mass exchange on a global scale, noting the importance of vertical transport through the Hadley cell and the large-scale eddies in the mid-latitudes. Danielsen derived a seasonally-dependent stratospheric mass outflow rate associated with large scale cyclogenesis, with a spring maximum rate three times the fall minimum rate [Danielsen and Mohnen, 1977].

Recently Holton [1990] and Rosenlof and Holton [1993] have estimated zonal mean ST mass exchange on a seasonal average basis. Holton [1990] utilized the "downward control" principle [Haynes and McIntyre, 1987] and mass continuity to estimate the seasonal-averaged zonal mean diabatic mass flow across the tropical tropopause into the stratosphere. The stated implication of the downward control principle is that the time and zonal mean downward mass flux across the extratropical tropopause is controlled by dynamical processes (associated with dissipating eddies) in the first few scale heights above the tropopause. Rosenlof and Holton [1993] added a zonal mean quasi-isentropic meridional transport across a model tropopause break (located at 30° N and 30° S) to arrive at a total mass flux into the stratosphere from the tropical troposphere. Their resulting turnover time for the extratropical portion of the stratosphere (adding both hemispheres together) between 200 mbar and 100 mbar was 8 months. By comparing with results from an estimate of a residual mean meridional circulation stream function (using the National Center for Atmospheric Research CCM2 model output), they found that the model result was a significantly shorter turnover time, namely 5 months. Although not an explicitly stated conclusion, their work indicates relatively higher ST exchange rates in the northern hemisphere and in the winter months,

Further understanding of the ST exchange budget is gained through studies which can elucidate the relative global-scale influence of physical processes which are not zonally symmetric and which include measurement time scales that extend from days to years. On "the scale of days to weeks, Hoerling et al. [1993] recently analyzed cross-tropopause mass exchange for the month of January, 1979, using the European Centre for Medium-Range Weather Forecasts (ECMWF) assimilated dataset for twice-daily evaluations of the synoptic tropopause. The global map of ST mass exchange thus produced clearly shows zonal asymmetry and the significant influence of. regional variability. Hoerling et al. [1993] indicate that the ST mass exchange in middle and subpolar latitudes is dominated by adiabatic transport along isentropes which cross the tropopause, and that the net outflow of stratospheric mass into the troposphere in the midlatitude bands significantly exceeds the inflow from the tropical latitudes. Mass balance is achieved due to mass flux into the stratosphere at high latitudes. The northern midlatitude region (2 5°N-50°N) extending from China across the Pacific through North America is a region of intense ST exchange during this time period, showing large areas of mass flux into the troposphere at rates which would deplete the overlying mass in the first scale height above the tropopause in less than a month.

Observational evidence of temporally dependent ST exchange on regional scales can be obtained with repetitive measurements of aerosol vertical profiles in the upper troposphere and lower stratosphere over multi-year periods. Such datasets can be used to intercompare with studies such as that reported by Hoerling et al. [1993] and place them in temporal context. The multi-year lidar dataset of upper tropospheric and lower stratospheric aerosol profiles over Pasadena, California, for example, can be used to estimate ST exchange rates which should be representative of the northern midlatitude belt, which is an active ST exchange region. Other long-term data sets from calibrated aerosol backscatter lidar measure-merits over Boulder, Colorado have been reported by Post [1986]. Long-term datasets from balloon-borne ***in-situ*** sensors over the Laramie, Wyoming site have been reported by Hofmann [1993] and Deshler et al. [1993].

As described below, the Pasadena location is favorable for observation of ST exchange rates and associated purging of stratospheric aerosol because the upper troposphere over this location is not strongly influenced by other tropospheric sources of optically active aerosol particles, e.g., convection of aerosol from regional continental sources. Given the prevailing air mass trajectories in the upper troposphere and lower stratosphere, the location is downstream of subtropical and midlatitude regions of the Pacific which are regions of intense outflow of stratospheric air into the upper troposphere, as pointed out by Hoerling, et al. [1993].

2. Measurement Methodology

The JPL backscatter lidar, which has been used for aerosol vertical profile measurements at wavelengths of 9.25 μm and 10,6 μm since 1984, has been described in detail previously [Menzies et al., 1984; Menzies et al., 1989]. Calibration issues have also been discussed in Kavaya and Menzies [1985]. The lidar is carefully calibrated using a hard target whose reflectance characteristics are linked to laboratory standards in order to produce tropospheric and lower stratospheric aerosol backscatter profiles in absolute units. For each vertical profile measurement a corresponding set of local boundary layer measurements are made in order to calculate the boundary layer extinction at the lidar wavelength. The extinction above the boundary layer can be modelled accurately enough to reduce the associated source of error to a relatively small value. The calibration methodology and the sensitivity of coherent detection CO_2 lidars at these relatively long infrared wavelengths is well suited for tropospheric and lower stratospheric measurements even in conditions of low aerosol loading. The lidar does not observe the molecular Rayleigh backscatter because of its extremely low level compared with the aerosol backscatter, even for very clean atmospheric conditions; consequently the use of the backscattering ratio technique to extract the aerosol contribution to the total backscatter does not apply. The backscattering ratio technique [Russell, et al., 1979], which has been extremely useful for stratospheric aerosol studies with shorter wavelength lidars, has well-known limitations in extracting aerosol information from the upper troposphere and lower stratosphere in clean conditions, when the aerosol backscatter is very small compared with the molecular Rayleigh backscatter.

Each lidar vertical profile of aerosol backscatter coefficient, $\beta\ (m^{-1} sr^{-1})$, includes data to a maximum altitude of 30 km, with a lidar vertical resolution of approximately 150 m. Except for periods of extreme volcanic activity, the backscatter signals from altitudes above 25 km are indistinguishable from the lidar receiver noise. For the purposes of assessing yearly averages and seasonal variations, the data are sorted into selected altitude regions, with a geometric mean β calculated for each region, as discussed in Menzies et al. [1989].

3. Observations

The data presented for the purpose of this study include the time period between January, 1985 and December, 1993, and the data are segregated into pre-Pinatubo and post-Pinatubo groups. The pre-Pinatubo period (Jan, 1985 through June, 1991) can be described as a relatively quiescent volcanic period, leadingto background aerosol mass conditions for the lower stratosphere [Hofmann, 1990]. In Figure 1 are plotted three 9.25 μm wavelength geometric mean β profiles which represent a wide range from very low to very high mass density of aerosol particles in the troposphere and lower stratosphere. These correspond to apre-Pinatubo (1985 through mid-1991) profile from thePasadenalidar, atwo-year (Oct. 1991 through Sept. 1993) post-Pinatubo profile also from the Pasadena lidar, and a profile representing the tropical Pacific region, taken with theJPLAirborne BackscatterLidar (MenziesandTratt, 1994) duringa spring 1990 GLOBE (Global Backscatter Experiment) Pacific circumnavigation mission on the NASA DC-8. The three profiles have in common the rapid decrease in β with increasing altitude in the lower troposphere, a region whose aerosol characteristics are significantly affected by convective mixing from below. The tropical Pacific profile indicates that the typical backscatter coefficient in the aircraft cruise altitude region (8-1 O km) is representative of the upper troposphere, above which the aerosol enhancement from the Kelut (8° S, 112° E) eruption of February, 1990 is evident. The Kelut aerosol plume is evident at tropical latitudes in the southern hemisphere in the Stratospheric Aerosol and Gas Experiment II (SAGE II) data of spring, 1990 [Kent, 1990] and remained evident through spring, 1991 [Trepte, et al., 1993]. ***In situ*** particle counter data from the GLOBE mission indicated extremely low aerosol mass concentrations (below 100 ng/m^3, occasionally dropping below 10 ng/m^3) in the equatorial free troposphere [Clarke, 1993]. Application of Mie scattering calculations to the lognormal size distribution curve fits of Clarke [1993] indicates that the particles in the 0.3 to 0.4 μm radius range contributed most to the lidar backscatter at the aircraft altitude. The post-Pinatubo profile indicates clearly the dramatic increase in aerosol backscatter from the lower stratosphere and the fact that during this period the lower stratosphere became the dominant source of large aerosol particles in the upper troposphere.

In Figure 2 the JPL lidar annually averaged aerosol backscatter coefficients (at the 9.25 μm wavelength) for four altitude bins are shown to provide further historical perspective. At the Pasadena, California lidar location, with the prevailing westerly flow in the free troposphere above, the altitudes above 5 km are relatively unaffected by surface sources of aerosol, as pointed out previously [Menzies et al., 1989]. The annually averaged atmospheric aerosol backscatter between 5 km and 20 km seemed to be in a steady state until 1989, when a significant decrease occurred, The low levels of β persisted until the Pinatubo plume reached 34° N 118° W in July, 1991. The data of Hofmann [1990] also indicate a drop in aerosol mixing ratio at the stratospheric maximum (between 18-22 km) beginning in 1988 and extending through 1990. The average upper tropospheric and lower stratospheric β levels during the 1989-90 period are within a factor of two of the average upper tropospheric β value observed with the JPL Airborne Backscatter Lidar in the tropical latitudes during the GLOBE 1989 and 1990 Pacific circumnavigation missions.

The seasonal variability in the aerosol backscatter as well as the coupling between the upper troposphere and lower stratosphere can be observed by sorting the pre-Pinatubo and post-Pinatubo lidar data into selected altitude regions of 5-km geometric thickness and then combining into monthly averages. These data are plotted on a 12-month scale for two altitude regions in Figures 3 and 4. Also on each of these figures is a least squares fit curve consisting of a combination of three Fourier terms: a constant, a 12-month period sinusoid, and a 6-month sinusoid. Regarding the pre-Pinatubo data set, the seasonal variability in the lower stratosphere is remarkably similar to that of the upper troposphere. The pronounced dip in the spring and slightly smaller dip in the autumn were observed in the earlier data of Menzies et al. [1989] for the upper troposphere. The large amplitude of the backscatter variation for both altitude regions, coupled with the in-phase relationship, strongly suggests tight coupling between the lower stratosphere and upper troposphere, with a mass exchange turnover time of three months or less during the early part of the year. The post-Pinatubo data set shown in Figure 3 also indicates strong coupling, especially during the winter and early spring when the upper tropospheric β level rises to nearly the same value as that of the lower stratosphere. Throughout this period the aerosol β at 9.25 μm wavelength was near 10-9 m^{-1} sr^{-1}, a value much higher than that in the unperturbed upper troposphere. With the assumption that the stratosphere is the predominant source of upper tropospheric aerosol (in the size range which dominates the lidar backscatter), a simple rate equation approach can be used to estimate the coupling rate, as discussed below.

4, Discussion

It is useful to first understand what particle size range is dominating the lidar backscatter for the pre- and post-Pinatubo conditions. Using the common Mie scattering assumption of spherical particles, the aerosol backscatter coefficient β (m^{-1} sr^{-1}) at the lidar wavelength λ can be expressed in terms of the particle size distribution, $n(r)dr$ and geometric cross section πr^2, as

$$\beta\ (180°) = (4\pi)^{-1} \int_0^\infty (\pi r^2)\, Q_{sca}(\lambda, r) P(180°) n(r) dr \qquad (1)$$

where $Q_{sca}(\lambda,r)$ is the scattering efficiency for a particle of radius r, and $P(180^o)$ is the phase function at the 180^0 backscatter angle. In the Rayleigh limit of small values of the size parameter, $2\pi r/\lambda$, the product of geometric cross section and scattering efficiency increases as r^6. For the lidar wavelength of 9.25 μm, the effective exponent for typical stratospheric sulfuric acid particles with radii between 0.2S and 1 μm lies between 5 and 6. Most analyses of the stratospheric aerosol size distributions have used the lognormal size distribution

$$n(r) = \frac{N_0}{\sqrt{2\pi} r \ln s} \exp\left(-\frac{(\ln(r/r_g))^2}{2(\ln s)^2}\right) \qquad (2)$$

where NO is the total number concentration, r_g is the median radius, and s is the geometric standard deviation, or multimodal variations of this form, The "effective radius" for the monomodal lognormal distribution is

$$r_{eff} = r_g \exp(2.5(\ln S)^2), \qquad (3)$$

Thomason [1991] chose a two-piece segmented power law model for the size distribution fit to SAGE II data, determining a best fit critical radius, below which the best fit value for the exponent in the power law falloff of $n(r)$ was near 2, and above which the best fit was in the range between 7 and 8.

Using the best fit values of r_g (0.05-0.1 μm) and s (-2) for various pre-Pinatubo size distribution measurements [Hofmann, 1990; Rosen and Kjome, 1991; Brogniez et al., 1992; Pueschel et al., 1993] in equation (1), one can conclude that particles with radii in the 0.2 -0.4 μm range contribute the most to the lidar backscatter coefficient, This is also in agreement with Thomason's [1991] best fit, for which the critical radius values ranged over values of 0.25 to 0.4 μm. With such a segmented power law distribution one can determine by inspection using equation (1) that the chief contributors to β are those particles at the critical radius. The range of radii which contributed most effectively to the lidar backscatter in the pre-Pinatubo lower stratosphere is effectively the same as that for the middle and upper troposphere in the low backscatter regions sampled during the GLOBE missions, using the Laser Optical Particle Counter data described by Clarke [1993] and also analyzed by Srivastava et al. [1992].

In contrast the post-Pinatubo size distributions obtained by Deshler et al. [1993], Pueschel et al. [1993], and Ansmann et al. [1993] were fit to bimodal or trimodal lognormal distributions. The larger modes are relatively narrow (s - 1.25-1.5), with the modal radii of the larger modes being substantially larger, in the range of 0.2-0.4 μm. The resulting range of particle radii for most effective contribution to the lidar backscatter is 0.7-1.0 μm. Although these particles are relatively large, sedimentation from an altitude of 20 km to the tropopause would require about one year. The lidar data indicate the presence of much faster mechanisms for mixing the stratospheric aerosol into the upper troposphere,

Considering only those aerosol particles in either the pre-Pinatubo or post-Pinatubo size range which dominates the contribution to lidar backscatter, we can use coupled rate equations for those aerosol populations in the lower stratosphere and upper troposphere to assess the ST exchange rate, Given the typical zonal winds and aerosol residence times in the upper troposphere and lower stratosphere, those populations sampled by the lidar over Pasadena are representative of a midlatitude belt stretching over the Pacific at upper tropospheric altitudes, and usually over a larger range of longitude at higher altitudes in the winter months. Using this simplified approach, we have

$$\frac{dN_2}{dt} = -N_2\gamma_{21} - W(N_2 - N_1) + R_2 \tag{4}$$

and

$$\frac{dN_1}{dt} = -N_1\gamma_{10} + N_2\gamma_{21} + W(N_2 - N_1) + R_1 \tag{5}$$

where N_2, N, are the level 2 (lower stratosphere) and level 1 (upper troposphere) populations, representing concentrations suitably weighted according to the value of the differential backscatter coefficient, $d\beta/d(ln(r/r_g))$; R_2 and R_1 are source terms; γ_{21} and γ_{10} are the respective decay rates from lower stratosphere to upper troposphere in the absence of mass mixing (e.g., due to sedimentation), and from upper troposphere to lower levels; and W is the ST mass exchange rate. The source term R_2 includes sedimentation from above, heterogeneous growth, and coagulation, and is heavily influenced by volcanic activity. The term R_1 includes sources other than from the stratosphere, i.e., from convective processes and quasi-isentropic transport, For upper tropospheric particles in the size range discussed here, nucleation scavenging in clouds is usually the dominant loss mechanism [Charlson and Rodhe, 1982; Lambert et al., 1983]. The scavenging varies considerably in space and time; however, a typical mean residence time $\tau_1 (= 1/\gamma_{10})$ - 10 days. The corresponding lower stratospheric residence times for the particles primarily responsible for the lidar backscatter, in the absence of ST mass exchange, are of the order of 600 days for the pre-Pinatubo size range and 200 days for the post-Pinatubo size range, i.e., $\gamma_{21} < \gamma_{10}$. The ST exchange mass balance assumed in equations (4) and (5) is appropriate for the entire northern hemisphere, but not likely to be a good assumption for the air masses sampled by the JPL lidar. This is discussed below in the context of applying the rate equations to interpret lidar observations.

Using these rate equations to describe the post-Pinatubo situation, in the absence of ST exchange, $N_2 > N_1$ due to the source term R_2 being unusually large. As the mixing (mass exchange) term becomes more dominant, the population difference decreases significantly. In the steady-state approximation we can express the population difference as

$$N_2 - N_1 = \frac{R_2\{1 - (\gamma_{21}/\gamma_{10})[1 + (R_1/R_2)]\}}{W + \gamma_{21}} \tag{6}$$

Since $\gamma_{21} < \gamma_{10}$, we can define an effective source term R, slightly reduced from R_2 to a value

$$R = R_2\left[1 - \frac{\gamma_{21}}{\gamma_{10}}\left(1 + \frac{R_1}{R_2}\right)\right] \tag{7}$$

Then the population difference can be expressed as

$$N_2 - N_1 = (R/\gamma_{21})\left[\frac{1}{1 + (W/\gamma_{21})}\right] \tag{8}$$

In this form the effect of the ST mass exchange term on the reduction of the population difference is apparent.

The lidar data of Figure 4 indicate a significant increase in the upper tropospheric aerosol backscatter during the winter and early spring, the β value rising nearly an order of magnitude over the four-month period when the ST exchange is expected to be most intense. The subsequent decay takes the β values down to the level typical of the pre-Pinatubo upper troposphere, implying that the sedimentation of the relatively large "lidar backscatter active" post-Pinatubo particles as a source from the lower stratosphere still has little effect on the upper tropospheric population, and that in the fall months the ST mixing term, even with N_2 values an order of magnitude larger than pre-Pinatubo values, has relatively little influence. During this time of year the N_1 population appears to be controlled by the tropospheric source and sink terms.

Using the data of Figure 4 we can estimate the size of the ST mass exchange rate, W, using the rate equations (4) and (5) after a few simplifying approximations are made. Although eqn. (8) provides at least a qualitative indication of the behavior of the populations, its direct use to provide a quantitative value of W is problematical because the assumption of steady-state conditions is not strictly valid, The rapid and very significant rise in N_1 indicates the dominance of the ST exchange term in equation (5) during the Jan-Apr period. At this point the second and fourth terms on the rhs of eqn. (5) have little significance. In Dec. -Jan., N_2 is about 10 times N_1; thus $W > 0.1\gamma_{10}$ during the succeeding months in order for the ST exchange term to affect the rate of change of N_1. Assuming Dec.-Jan, initial conditions, integration of the rate equations over the succeeding three months results in a value of W = 0.023 day-l. (The source term R_2 was given a time-dependent term during the integration period to mimic the observed behavior of N_2.) This result is approximate, given the fluctuation level of the data points. Since it requires approximately 220 days for a 0.8 μm radius particle to sediment down through the 14-18 km layer, the value of W calculated above results in a ratio $(W/\gamma_{21}) \approx$ 5-6 for the winter and early spring conditions. Later in the year, as stated above, the ST mixing term in eqn. (5) becomes much less significant. Since $N_2 \approx 10N_1, W < 0.1\gamma_{10}$, i.e., the mass exchange or turnover time is greater than 100 days during this period.

If the results of Hoerling, et al. [1993] for January, 1979 can be generalized, then the assumption of mass exchange balance for mid-latitude air masses (i.e., a single exchange rate, W) is not valid, for they point out that there is a significant net mass influx into the troposphere for this month. However, for post-Pinatubo conditions N_2 is much larger than N_1 except for the months of April and May, and the impact of a smaller rate for mass flow into the stratosphere on the above conclusions is minor.

Applying the rate equation approach to the lidar data for pre-Pinatubo conditions requires further development; nonetheless, equations (4) and (5) can be used to draw qualitative conclusions from the lidar data, The sedimentation rate γ_{21} decreases by a factor of approximately ‘three because the primary contributors to the lidar backscatter are much smaller particles. The lower stratospheric source term R_2 is also much smaller. The relatively large value of W in eqn. (4) results in the ST mixing term forcing $(N_2 - N_1)/N_2$ to be relatively small, at least through the winter/spring months, The fact that the seasonal cycle in N_1 is out of phase with that of the lower tropospheric "lidar backscatter-active" aerosol population, which peaks in the spring and early summer, implies that the source term R_1 is relatively weak at these altitudes, and it is being dominated by a seasonally dependent purging process. The purging in the winter-spring period is likely associated with the intense jet stream, the increased tendency for large scale cyclogenesis, and the formation of high clouds and precipitation in the cyclonic cores. The “makeup” air mass injected into the lower stratosphere of the northern midlatitude belt from the tropical upper troposphere (whose flux is maximum in the winter months according to Rosenlof and Holton [1993]) is likely to be relatively devoid of lidar backscatter-active aerosol particles, as found by Clarke [1 993] and the GLOBE lidar results as indicated in Figure 1.

5. Conclusions

It has been shown that stratosphere-troposphere exchange processes significantly affect the seasonal behavior of the JPL lidar aerosol backscatter at upper tropospheric and lower stratospheric altitudes. The post-Pinatubo seasonal behavior clearly shows significant exchange taking place during the winter and early spring, leading to a large influx of aerosol mass into the troposphere, where the aerosol residence times are relatively short. The histories of the air masses sampled by the lidar at the Pasadena location in the altitude range discussed here are predominantly associated with the 25°N to 50°N latitude belt which reaches back over the Pacific to the east coast of Asia, a region which Hoerling, et, al. [1993] point out as a region of very large outflow of stratospheric air mass across the tropopause in their January 1979 case study. (The Hoerling et al. [1993] case study also shows a more localized region of intense flow into the stratosphere just off the coast of the southwestern U. S., a nearly horizontal flow from tropical latitudes across the sloping tropopause, or tropopause break.) With the aid of a rate equation approach to describe the kinetics of the upper tropospheric and lower stratospheric populations, a value for the winter-spring ST mass exchange rate was derived from the lidar data. The result indicates a mass exchange time of approximately 45 days during the winter-spring period, An upper limit was also derived for the exchange rate in the fall, leading to the conclusion that the exchange time is greater than 100 days during this period. This seasonal variation is consistent with estimates by Danielsen and Mohnen [1977] and Holton [1990] of a 3:1 ratio between the maximum and minimum flux rates.

The ST mass exchange rate derived from the lidar data for the winter and early spring is about a factor of two higher than that which can be derived from the zonal mean Rosenlof and Holton [1993] results (using the CCM2 model output) for the residence time of the northern extratropical region between 100 mbar and 200 mbar. It appears to be consistent with the results of Hoerling et al. [1993] in their January, 1979 case study. Extension of this kind of study to additional months which overlap the relevant lidar data is certainly desirable.

This study underscores the conclusion that the purging of the Pinatubo aerosol is dominated by ST exchange, rather than sedimentation, at least in the northern midlatitude region, A corollary is that the purging is seasonally dependent, and attempts to estimate stratospheric aerosol decay times based on long-term data sets must take this into account. From the ST exchange rates derived here, one can conclude that the Pinatubo aerosol purging during the months Jan.-April contribute more than half the yearly total. Extrapolating the derived value of the winter month ST exchange rate, W, to the entire northern hemisphere 25°-500 latitude belt, the purging rate of the global stratospheric aerosol mass, M, due to this mechanism alone is

$$-\frac{1}{M}\frac{dM}{dt} \approx 2 \times 10^{-3} \; per \;\; day$$

during the - 100 day period of intense exchange, assuming that approximately half the Pinatubo column aerosol mass resides in the altitude region below 18 km which is observed to be participating in the ST exchange. The seasonal dependence of the ST exchange should impact seasonal variability of cirrus formation at northern midlatitudes in periods of high volcanic influence, due to the impact of high aerosol flux across the tropopause [Sassen, 1992]. The seasonal variability of the ST mass exchange rate also has important implications in assessments of the impact of both subsonic and supersonic aircraft [e.g., Douglass, et al., 1993] on the chemistry of the lower stratosphere and upper troposphere. It is important in this regard to include the significant zona asymmetries which are likely.

Acknowledgements

The authors would like to acknowledge helpful discussions with R. Zurek and J. Margitan at JPL, and M. J. Post of the NOAA Environmental Technology Laboratory. This work was carried out by the Jet Propulsion Laboratory, California Institute of Technology, under contract with the National Aeronautics and Space Administration.

REFERENCES

Ansmann, A., U. Wandinger, and C. Weitkamp, One-year observations of Mount-Pinatubo aerosol with an advanced Raman lidar over Germany at 53.5° N, *Geophys. Res. Lett.,* 20, 711-714, 1993.

Brogniez, C., R. Santer, B.S. Diallo, M. Herman, and J. Lenoble, Comparative observations of stratospheric aerosols by ground-based lidar, balloon-borne polarimeter, and satellite solar occultation, *J. Geophys. Res., 97, 20,805-20,823, 1992.*

Browell, E. V., E.F. Danielsen, S. Ismail, G.L. Gregory, and S.M. Beck, Tropopause fold structure determined from airborne lidar and in situ measurements, *J. Geophys. Res., 92, 2112-2120,* 1987.

Clarke, A.D., Atmospheric nuclei in the Pacific midtroposphere: their nature, concentration, and evolution, *J. Geophys. Res., 98, 20,633-20,647, 1993.*

Danielsen, E. F., Stratospheric-Tropospheric exchange based on radioactivity, ozone, and potential vorticity, *J. Atmos. Sci., 25, S02-5 18, 1968.*

Danielsen, E.F., and V.A. Mohnen, Project Duststorm report: Ozone transport, in situ measurements, and meteorological analyses of tropopause folding, *J. Geophys. Res., 82, 5867-5877, 1977.*

Danielsen, E. F., R.S. Hipskind, S.E. Gaines, G.W. Sachse, G.L. Gregory, and G.F. Hill, Three-dimensional analysis of potential vorticity associated with tropopause folds and observed variations of ozone and carbon monoxide, ***J. Geophys. Res., 92,2103-2111, 1987.***

Deshler, T., B.J. Johnson, and W.R. Rozier, Balloonborne measurements of Pinatubo aerosol during 1991 and 1992 at 41° N: vertical profiles, size distribution, and volatility, ***Geophys. Res. Lett., 20, 1435-1438,*** 1993.

Hoerling, M. P., T.K. Schaack, and A.J. Lenzen, A global analysis of stratospheric-tropospheric exchange during northern winter, ***Mon. Wea. Rev., 121,162-172,*** 1993.

Hofmann, D. J., Increase in the stratospheric background sulfuric acid aerosol mass in the past 10 years, ***Science, 248, 996-1000, 1990.***

Hofmann, D. J., Twenty years of balloon-borne tropospheric aerosol measurements at Laramie, Wyoming, ***J. Geophys. Res., 98, 12,753-12,766, 1993.***

Holton, J. R., On the global exchange of mass between the stratosphere and troposphere, *J. Atmos. Sci., 47, 392-395, 1990.*

Jensen, E.J., and O.B. Toon, "The potential effects of volcanic aerosols on cirrus cloud microphysics", *Geophys. Res. Lett., 19, 1759-1762, 1992.*

Kavaya, M.J., and R.T. Menzies, Lidar aerosol backscatter measurements: systematic, modeling, and calibration error considerations, *Appl. Opt., 24, 3444-3453, 1985.*

Kent, G. S., NASA Langley Research Center, Hampton, VA, personal communication, 1990.

Kritz, M., S.W. Rosner, E.F. Danielsen, and H.B. Selkirk, Air mass origins and troposphere-to-stratosphere exchange associated with mid-latitude cyclogenesis and tropopause folding inferred from ^{7}Be measurements, *J. Geophys. Res.,* 96, 17,405-17,414, 1991.

Lacis, A., J. Hansen, and M. Sate, "Climate forcing by stratospheric aerosols", *Geophys. Res. Lett., 19, 1607-1610, 1992.*

Lambert, G., J. Sanak, and G. Polian, Mean residence time of the submicrometer aerosols in the global troposphere, in Precipitation Scavenging, Drv Deposition, and Resuspension, vol. 2, edited by H. R. Pruppacher, R. G. Semonin, and W. G, N. Slinn, pp. 1353-1359, Elsevier, New York, 1983.

McCormick, M. P., T.J. Swissler, W.P. Chu, and W.H. Fuller, Jr., Post-volcanic stratospheric aerosol decay as measured by lidar, *J. Atmos. Sci.,* 35, 1296-1303, 1978.

Menzies, R. T., M.J. Kavaya, P.H. Flamant, and D.A. Haner, Atmospheric aerosol backscatter measurements using a tunable coherent CO_2 lidar, *Appl. Opt, 23, 2510-2516, 1984.*

Menzies, R.T., G.M. Ancellet, D.M. Tratt, M.G. Wurtele, J.C. Wright, and W.Pi, 1989: Altitude and seasonal characteristics of aerosol backscatter at thermal IR wavelengths using lidar observations from coastal California, *J. Geophys. Res.,* 94, 9897-9908.

Menzies, R. T., and D.M. Tratt, Airborne CO_2 coherent lidar for measurements of ‘ atmospheric aerosol and cloud backscatter, *Appl. Opt., 33, 1994,* to be published.

Porter, J. N., A.D. Clarke, G. Ferry, and R.F. Pueschel, Aircraft studies of size-dependent aerosol sampling through inlets, *J. Geophys. Res.,* 97,3815-3824, 1992.

Post, M.J., Atmospheric purging of El Chichon debris, *J. Geophys. Res., 91*, 5222-5228, 1986.

Pueschel, R. F., S.A. Kinne, P.B. Russell, and K.G. Snetsinger, Effects of the 1991 Pinatubo volcanic eruption on the physical and radiative properties of stratospheric aerosols, ***IRS*** ’92: ***Current Problems in A tmospheric Radiation,*** Proc. International Radiation Symposium, A. Deepak, Hampton, VA, 1993.

Reiter, E. R., Stratospheric-tropospheric exchange processes, Rev. *Geophys. Space Phys., 13, 459-474, 1975.*

Rosen, J. M., and N.T. Kjome, Backscattersonde: a new instrument for atmospheric aerosol research, *Appl. Opt.,* 30, 1552-1561, 1991.

Rosenlof, K, H., and J.R. Holton, Estimates of the stratospheric residual circulation using the downward control principle, *J. Geophys. Res.,* 98, 10,465-10,479, 1993.

Russell, P. B., T.J. Swissler, and M.P. McCormick, Methodology for error analysis and simulation of lidar aerosol measurements, *Appl. Optics, 18, 3783-3797, 1979.*

Russell, P. B., E.F. Danielsen, R.A. Craig, and H.B. Selkirk, The NASA Spring 1984 Stratosphere-Troposphere Exchange Experiment: science objectives and operations, *J. Geophys. Res.,* 96, 17,401-17,404, 1991.

Sassen, K., Evidence for liquid-phase cirrus cloud formation from volcanic aerosols: climatic implications, *Science,* 257, 516-519, 1992.

Shapiro, M. A., Turbulent mixing within tropopause folds as a mechanism for the exchange of chemical constituents between the stratosphere and troposphere, *J. Atmos. Sci., 37, 994-1004,* 1980.

Staley, D. O., On the mechanism of mass and radioactivity transport from stratosphere to troposphere, *J. Atmos. Sci., 19*, 450-467, 1962, Thomason, L. W., A diagnostic stratospheric aerosol size distribution inferred from SAGE II measurements, J. Geophys. Res., 96, 22,501-22,508, 1991.

Trepte, C. R., R.E. Veiga, and M.P. McCormick, The poleward dispersal of Mount Pinatubo volcanic aerosol, *J. Geophys. Res.*, 98, 18,563-18,573, 1993.

Tuck, A. F., E.V. Browell, E.F. Danielsen, J.R. Holton, B.J. Hoskins, D.R. Johnson, D. Kley, A.J. Krueger, G. Megie, R.E. Newell, and G. Vaughan, Stratospheric-Tropospheric Exchange, Chapter 5, ***Atmospheric Ozone: 1985***, World Meteorological Organization, Report No. 16.

Wei, M.-Y., A new formulation of the exchange of mass and trace constituents between the stratosphere and troposphere, ***J. Atmos. Sci., 44, 3079-3086, 1987.***

Weisenstein, D. K., M.K.W. Ko, J.M. Rodriguez, and N.-D. Sze, Impact of heterogeneous chemistry on model-calculated ozone change due to high speed civil transport aircraft, *Geophys. Res. Lett., 18*, 1991-1994, 1991.

FIGURE CAPTIONS

Figure 1. Profiles of geometric mean aerosol backscatter coefficient for pre-Pinatubo and post-Pinatubo conditions above the Pasadena, CA lidar site, and spring, 1990 tropical (20°S - 20°N) Pacific conditions from airborne lidar data.

Figure 2. Multi-year plot of annual geometric mean aerosol backscatter coefficient in four altitude bands.

Figure 3. Monthly mean backscatter coefficients for two altitude regions: 8-13 km (upper troposphere), and 14-18 km (lower stratosphere). These monthly mean values include data from the years 1985 through mid-1991, corresponding to pre-Pinatubo conditions.

Figure 4. Monthly mean backscatter coefficients for the same altitude regions as in Figure 3, for the period October, 1991 through September, 1993, corresponding to post-Pinatubo conditions,

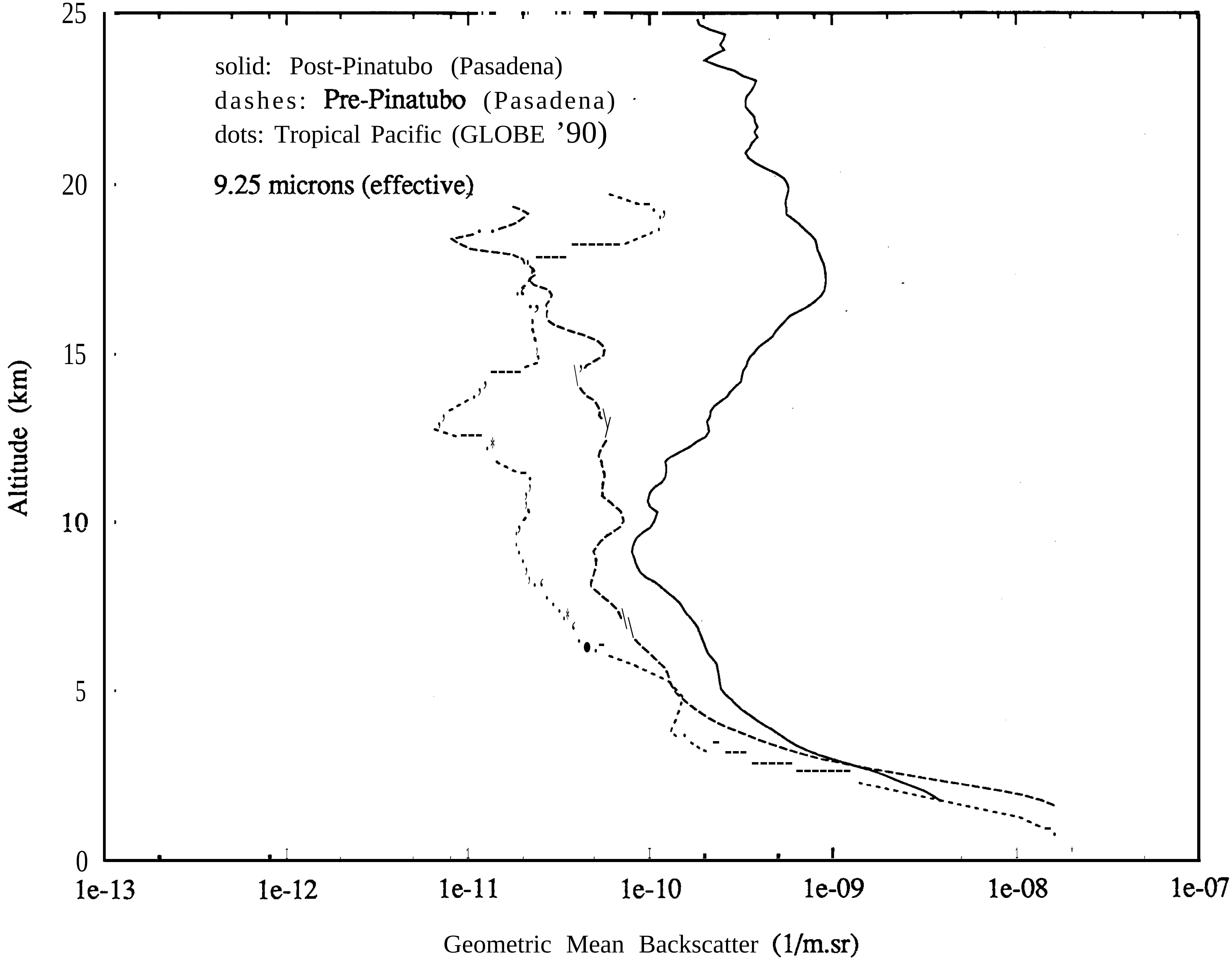
solid: Post-Pinatubo (Pasadena)
dashes: Pre-Pinatubo (Pasadena)
dots: Tropical Pacific (GLOBE '90)
9.25 microns (effective)
Altitude (km)
0
5
10
15
20
25
1e-13
1e-12
1e-11
1e-10
1e-09
1e-08
1e-07
Geometric Mean Backscatter (1/m.sr)

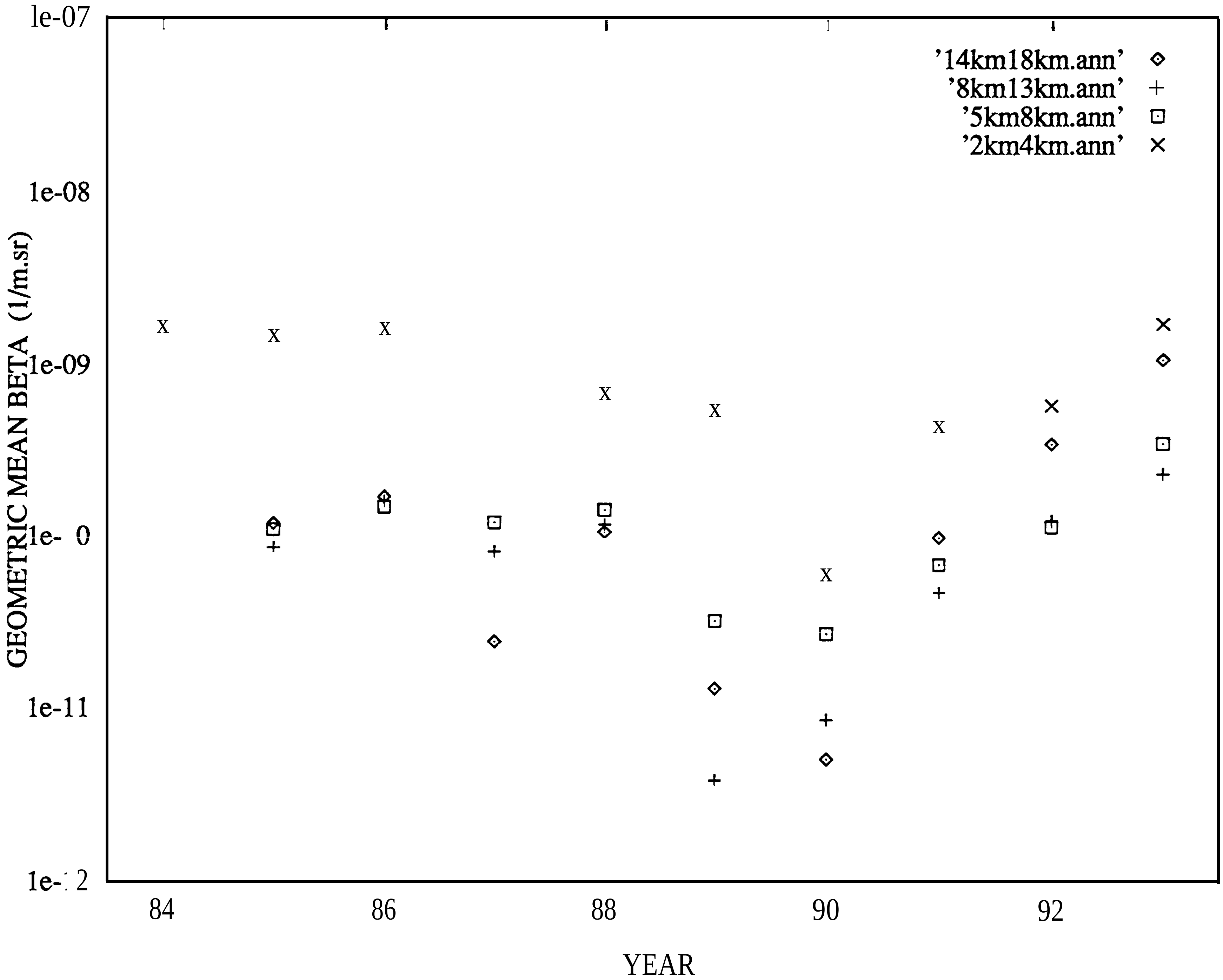

'14km18km.ann'
'8km13km.ann'
'5km8km.ann'
'2km4km.ann'
le-07
1e-08
1e-09
1e- 0
1e-11
1e-: 2
GEOMETRIC MEAN BETA (1/m.sr)
84
86
88
90
92
YEAR

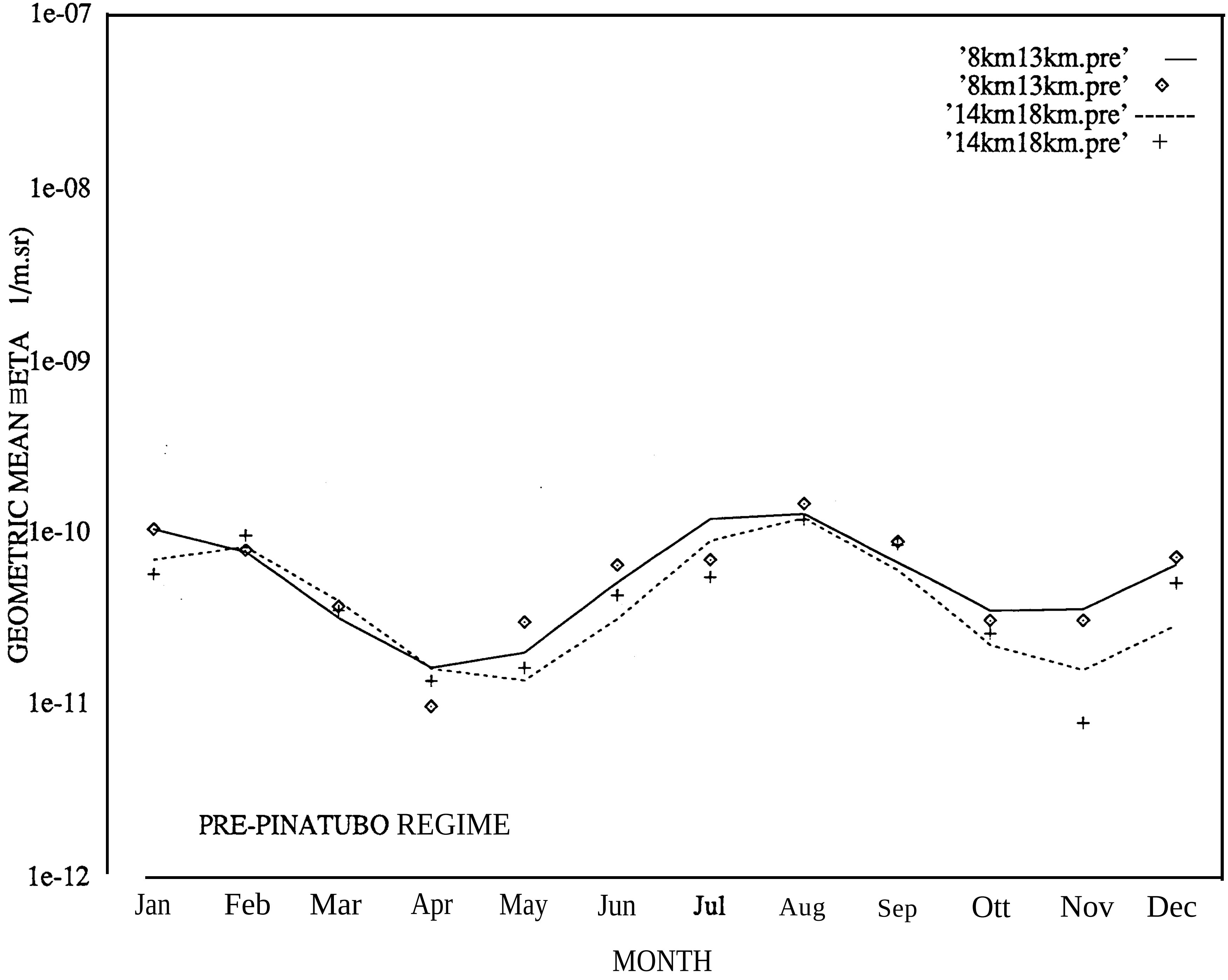

1e-07
1e-08
1e-09
1e-10
1e-11
1e-12
GEOMETRIC MEAN BETA 1/m.sr)
'8km13km.pre'
'8km13km.pre'
'14km18km.pre'
'14km18km.pre'
PRE-PINATUBO REGIME
Jan
Feb
Mar
Apr
May
Jun
Jul
Aug
Sep
Ott
Nov
Dec
MONTH

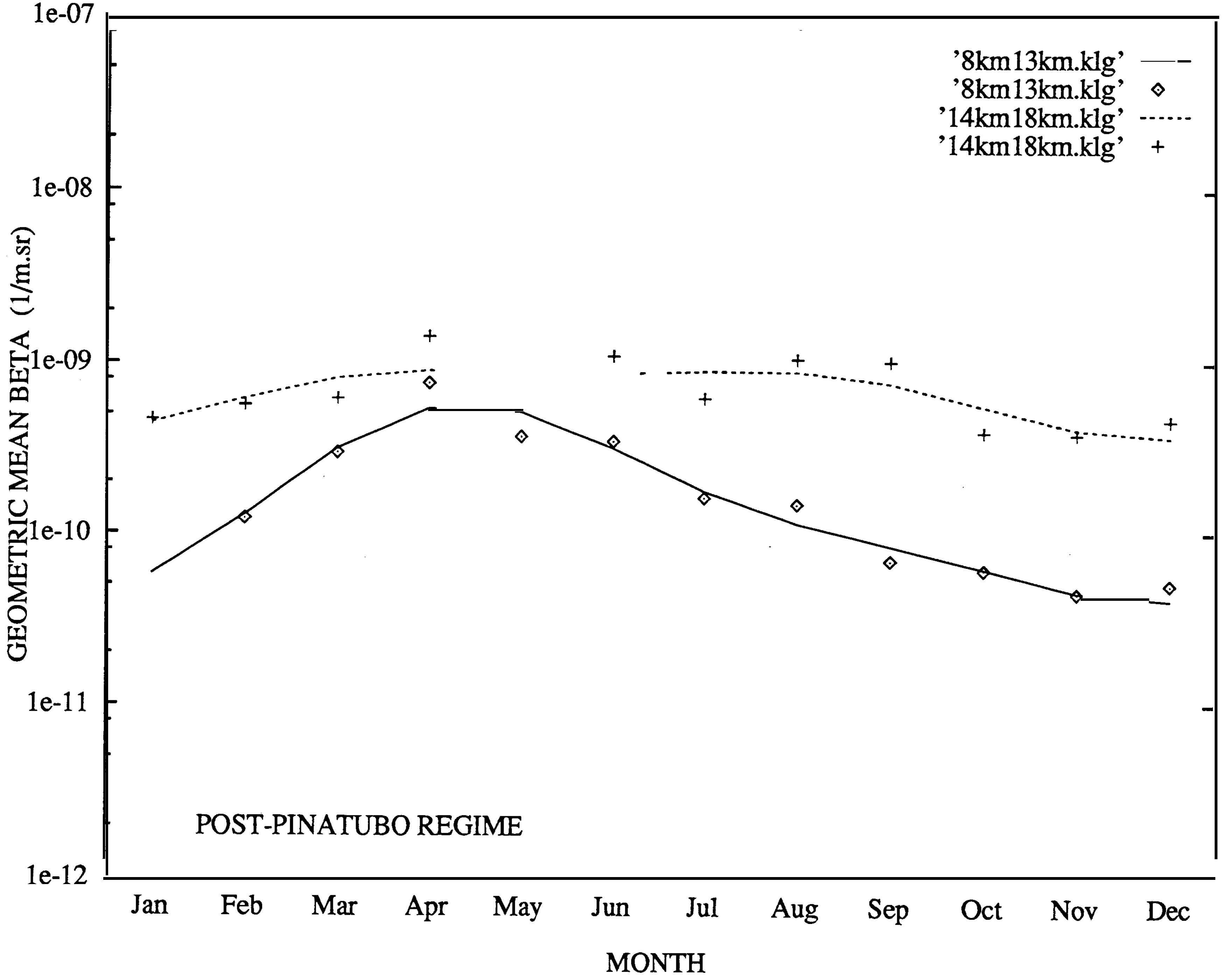
'8km13km.klg'
'8km13km.klg'
'14km18km.klg'
'14km18km.klg'
1e-07
1e-08
1e-09
1e-10
1e-11
1e-12
GEOMETRIC MEAN BETA (1/m.sr)
POST-PINATUBO REGIME
Jan
Feb
Mar
Apr
May
Jun
Jul
Aug
Sep
Oct
Nov
Dec
MONTH